
Digital Communications 2

Directed and Practical Work

Safwan El Assad
Dominique Barba

Color Section

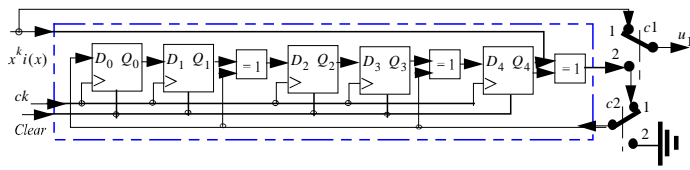
Group g	$p(g)_0$	$p(g)_1$	Code
g_1	0.6	0.6	0
g_2	0.3	0.4	1
g_3	0.1		11

Group g_1	Code
c_0	0 0 0
c_1	0 0 1
c_2	0 1 0
c_3	0 1 1

Group g_2	Code
c_4	1 0 0 0
c_5	1 0 0 1
c_6	1 0 1 0
c_7	1 0 1 1

Group g_3	Code
c_8	1 1 0 0 0
c_9	1 1 0 0 1
c_{10}	1 1 0 1 0
c_{11}	1 1 0 1 1
c_{12}	1 1 1 0 0
c_{13}	1 1 1 0 1
c_{14}	1 1 1 1 0
c_{15}	1 1 1 1 1

Table 1.6. Construction of Huffman code C_2



$c1c2$	ck	$i(x)$	D_0	Q_0 D_1	Q_1	D_2	Q_2 D_3	Q_3	D_4	Q_4	u_1
1 1				0	0					0	1
		1×8		1	0	1	0	0	1	0	1
	1°										
	0			1	1	1	1	0	1	1	0
	2°										
	1			0	1	1	1	1	1	1	1
	3°										
	0			1	0	1	0	1	0	0	0
	4°										
	0			0	1	0	1	0	1	1	0
	5°										
	1			0	0	0	1	0	0	1	1
	6°										
	0			0	0	0	0	1	0	0	0
	7°										
	1			1	0	1	0	0	0	0	1
	8°										
	1			1	1	1	1	1	1	1	1
	9°										
2 2	0			0	1	0	1	1	1	1	1
	10°										
	0			0	0	0	0	1	1	1	1
	11°										
	0			0	0	0	0	0	1	1	1
	12°										
	0			0	0	0	0	0	1	1	1
	13°										
	0			0	0	0	0	0	0	0	1
	14°										

Table 1.15. Description of the operations of the premultiplied coder

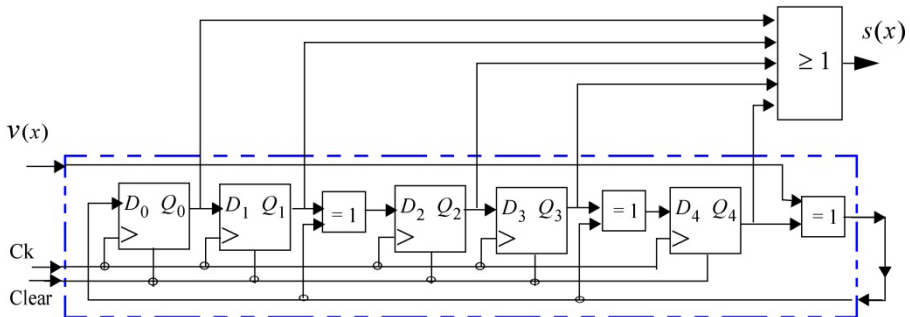


Figure 1.14. Structure of the decoder for the detection of errors

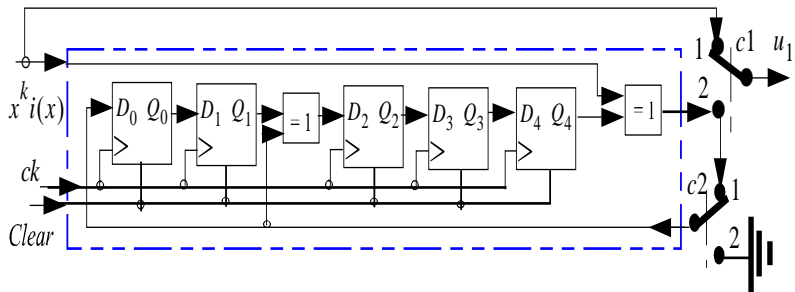


Figure 1.17. Implementation scheme of the coder

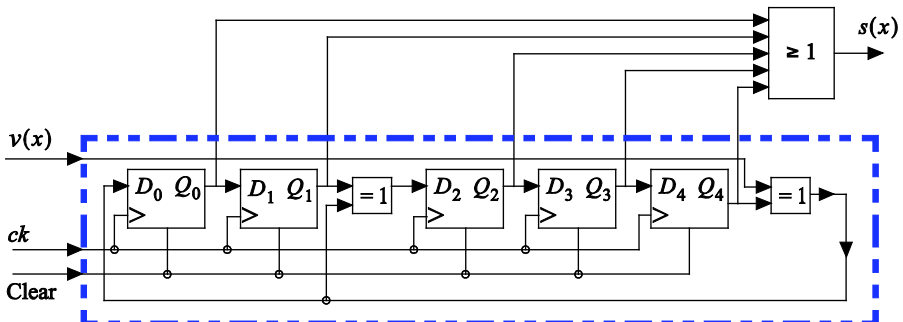


Figure 1.18. Implementation scheme of the decoder

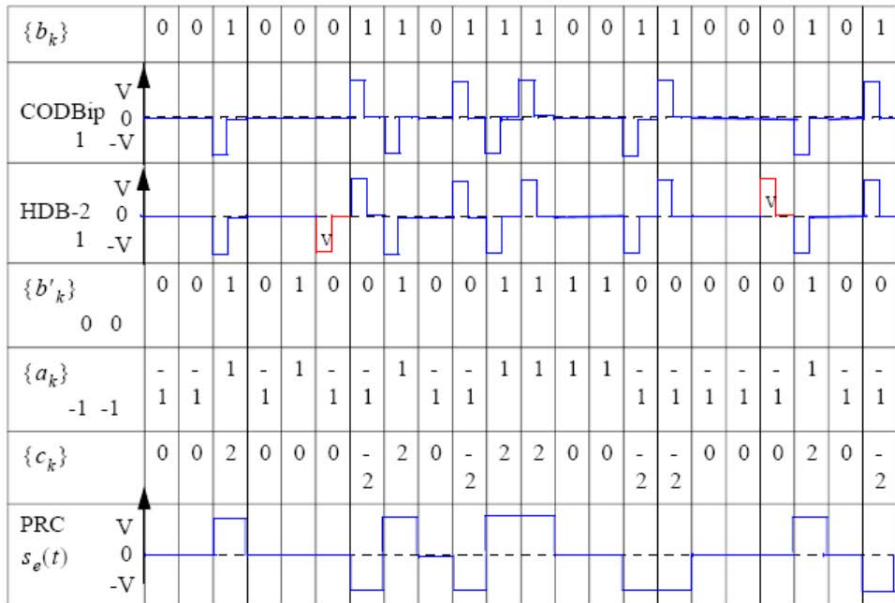


Table 2.4. Chronograms of the signals and coded symbols

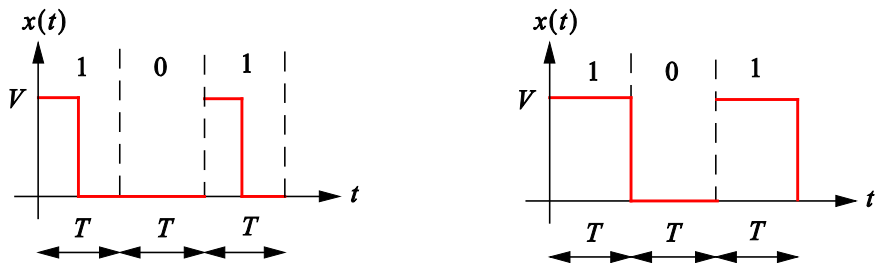


Figure 2.2. Examples of binary RZ and NRZ codes

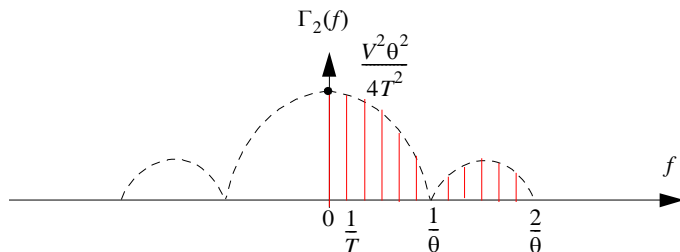


Figure 2.8. Discrete spectral components of the power spectral density $\Gamma_2(f)$

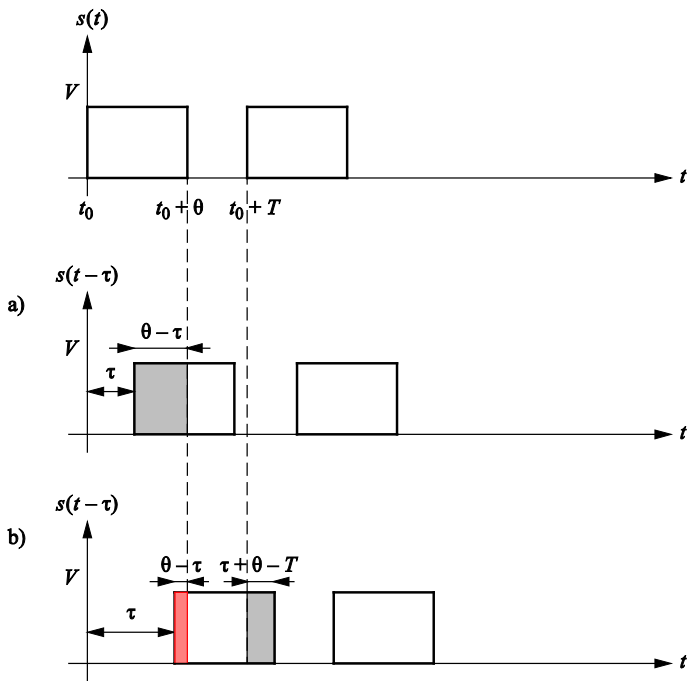


Figure 2.9. First situation: $0 < \tau \leq \theta$ (with $T/2 < \theta \leq T$)

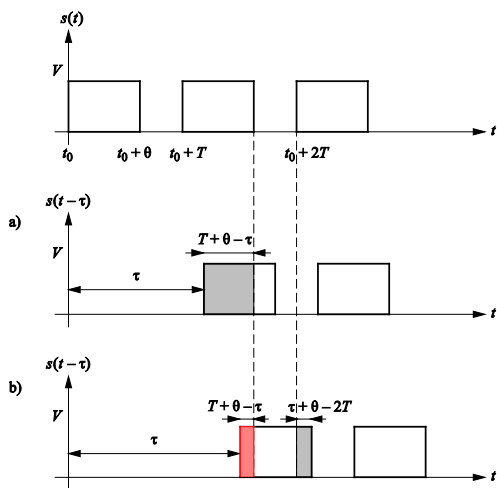


Figure 2.11. Third situation: $T \leq \tau < T + \theta$

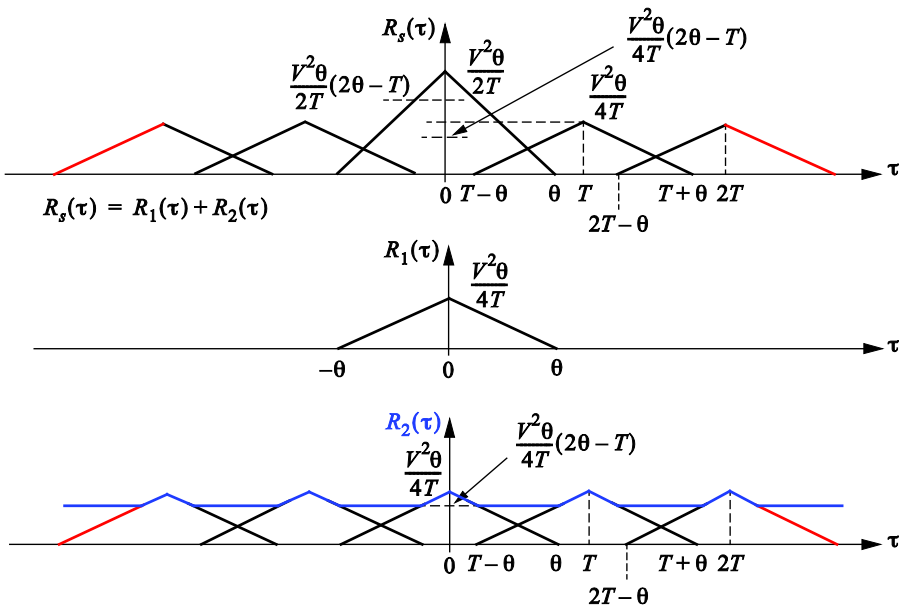


Figure 2.12. Autocorrelation function $R_s(\tau)$ and its decomposition

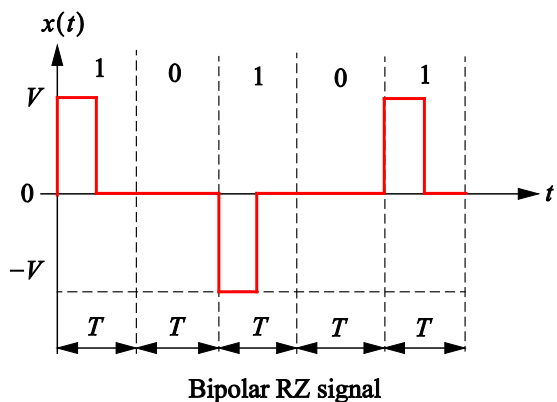


Figure 2.13. Example of a bipolar RZ signal waveform

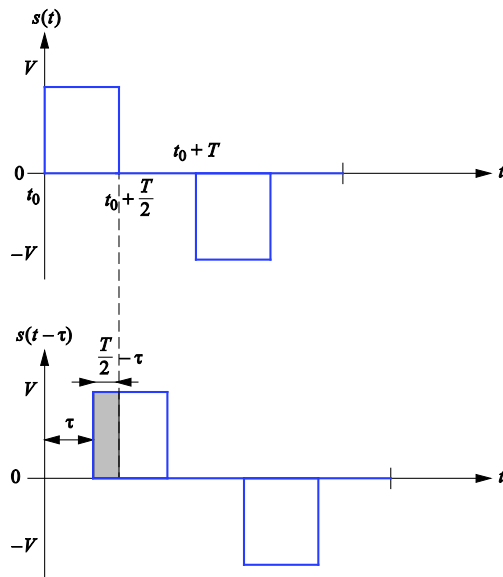


Figure 2.14. First case: $0 < \tau < T/2$ and a positive impulsion at t

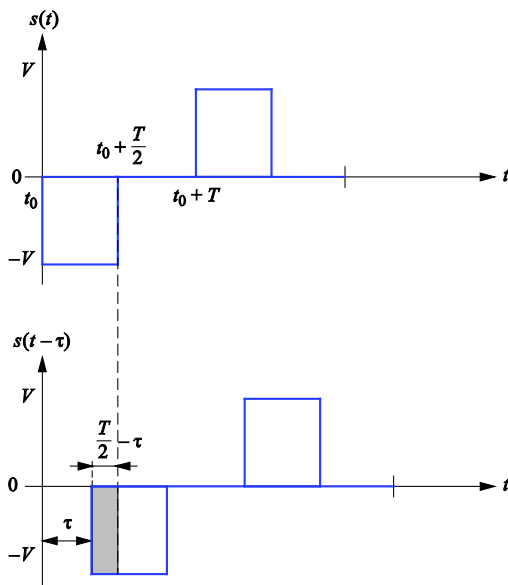


Figure 2.15. First case: $0 \leq \tau \leq T/2$ and negative impulse at t

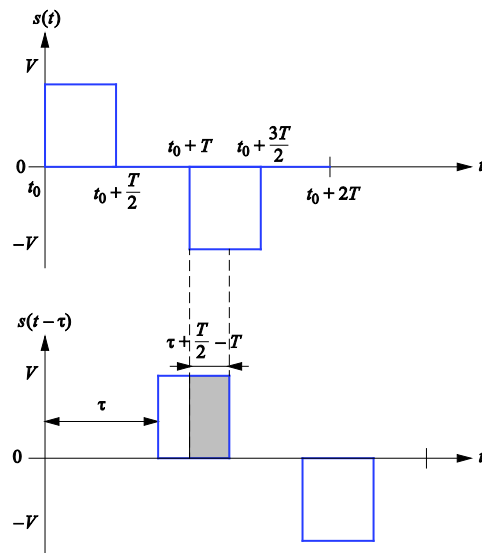


Figure 2.16. Second case: $T/2 < \tau \leq T$

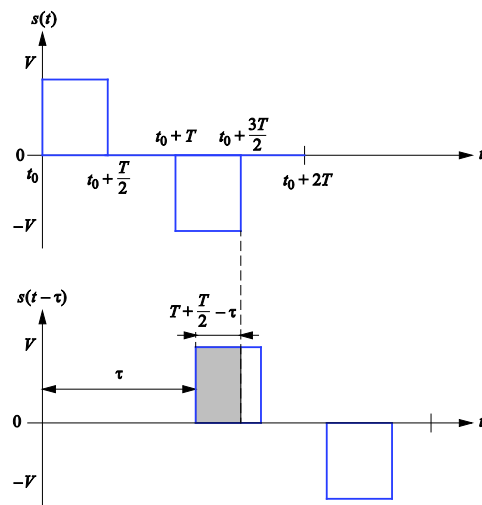


Figure 2.17. Third case: $T < \tau \leq T + T/2$

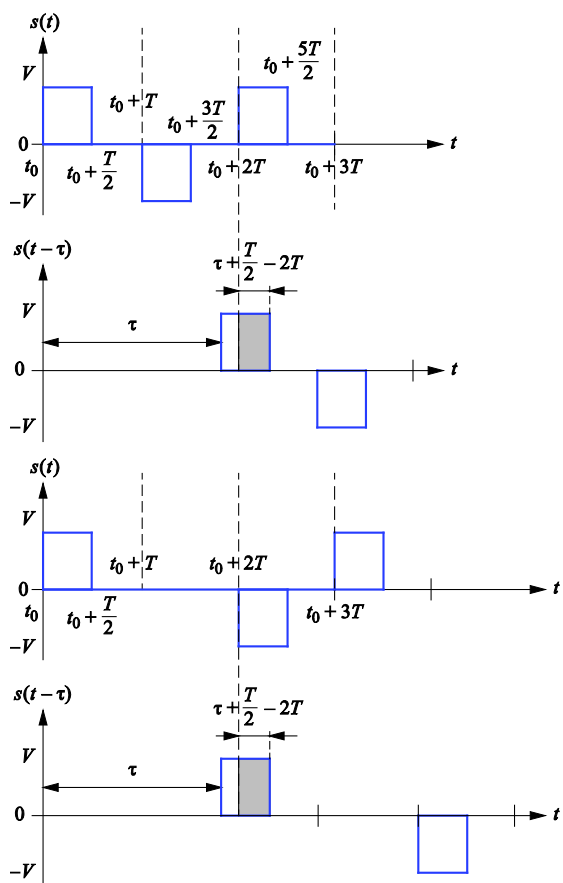


Figure 2.18. Fourth case: $3T/2 < \tau \leq 2T$

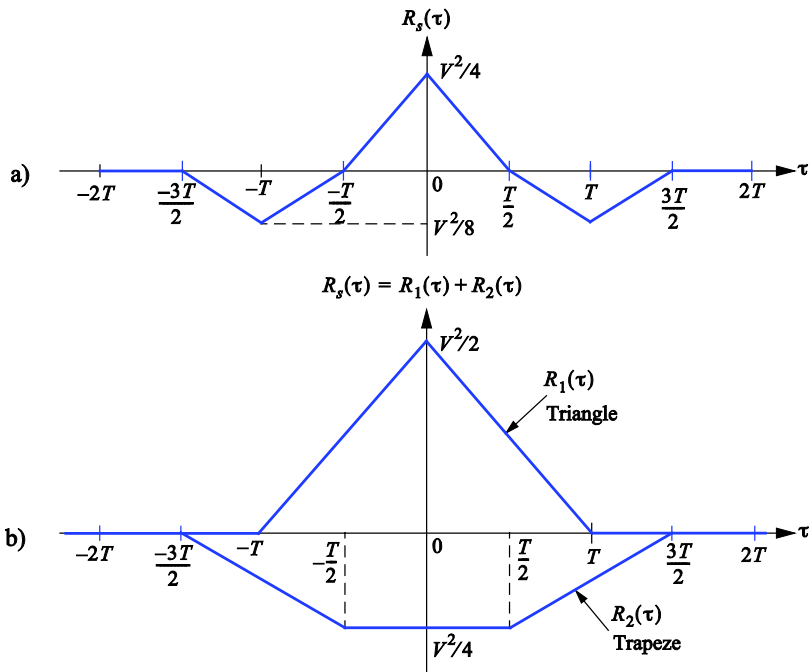


Figure 2.19. (a) Autocorrelation function of the bipolar RZ code and
(b) its decomposition into the sum of two functions

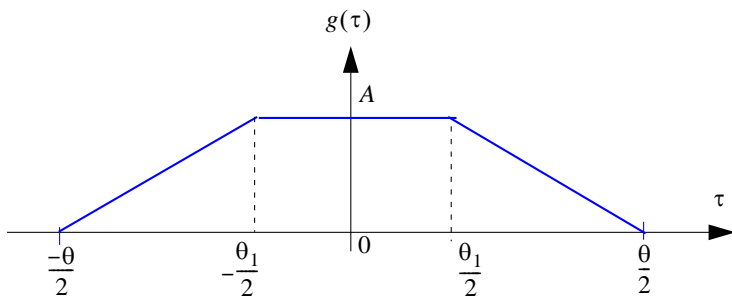


Figure 2.20. Trapezoidal function

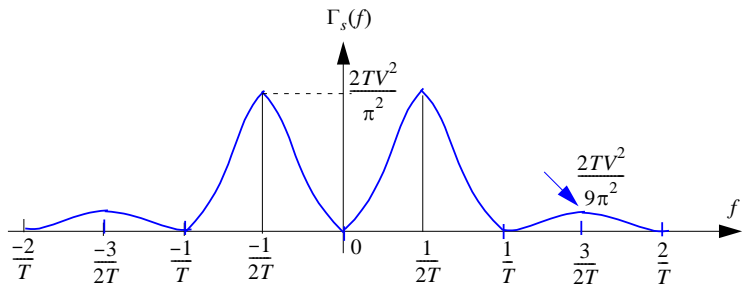


Figure 2.21. Power spectral density of the bipolar RZ code

$\{b_n\}$	0 0 0 0 1 0 1 1 0 1 0 0 0 1 1 1 1 0 1 0 0 0
$\{b'_n\}$	0 0 0 0 1 0 0 1 0 0 0 0 0 1 1 0 1 1 1 1 1 1
$\{a_n\}$	- - - - 1 - - 1 - - 1 - - 1 1 1 - - 1 1 1 1 1 1 1
$\{-1 -1\}$	1 1
$\{c_n\}$	0 0 0 0 2 0 - 2 2 0 - 2 0 0 0 2 2 - 2 0 2 0 0 0
$s_e(t)$	V 0 -V

Table 2.5. Chronogram of the time sequence and of the transmitted signal

$\{b_n\}$	1 0 0 0 0 0 V + 1 1 0 B - 0 0 0 V - 0 1 1 0 B + 0 0 0 V + 0 1 0
$s_{HDB-3}(t)$	V 0 -V

With V: polarity alternation violation bit (bit of violation); B: stuffing bit.

Table 2.6. Generation of the HDB-3 signal and chronogram

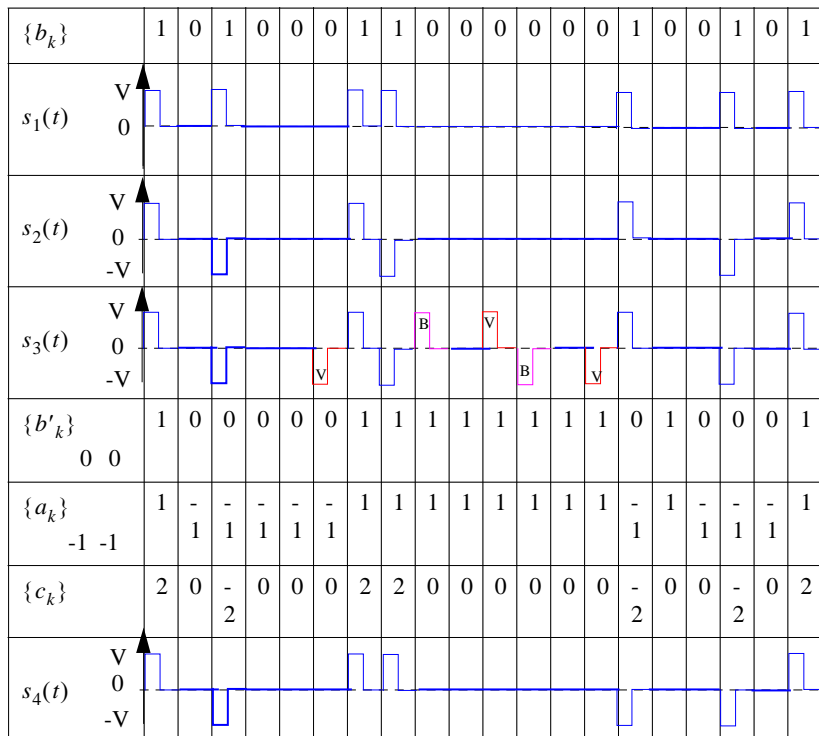


Table 2.7. Temporal representations of the different signals

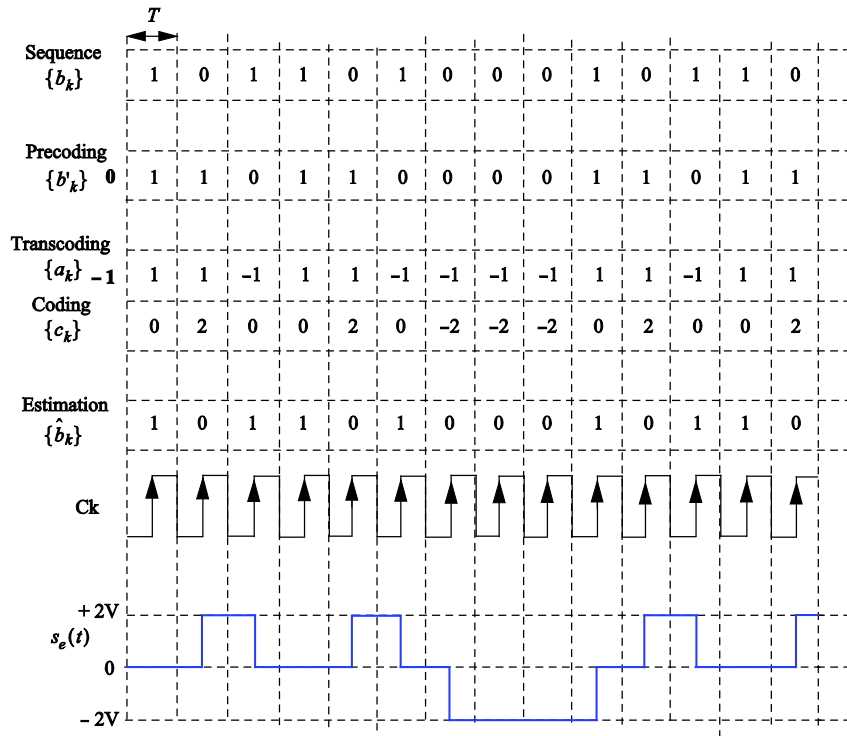


Figure 2.45. Chronograms of duobinary coding and decoding

$\{b_k\}$				1	0	0	1	0	1	1	1	1	0	1	0	0	1	0
b'_k	0	0	0	1	0	0	0	0	1	1	1	1	1	0	1	1	1	1
$\{a_k\}$	-1	-1	-1	1	-1	-1	-1	-1	1	1	1	1	-1	1	1	1	1	1
$\{c_k\}$				2	0	0	-2	0	2	2	2	2	0	-2	0	0	2	0
$\{\hat{b}_k\}$				1	0	0	1	0	1	1	1	1	0	1	0	0	1	0
$s_e(t)$				V	0	$-V$		V	0	$-V$		V	0	$-V$		V	0	$-V$

Table 2.31. Temporal sequences

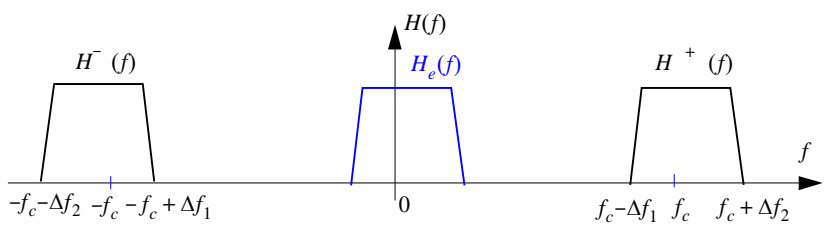


Figure 3.2. Supports of transfer function $H(f)$ and $H_e(f)$